

Theses of Doctoral (Ph.D.) Dissertation

**Evaluation and development of water flow
parameters for precision irrigation technology**

Andrea Szabó
Ph.D. candidate

Dissertation supervisor:
Prof. Dr. Attila Nagy



UNIVERSITY OF DEBRECEN
Doctoral School of Nutrition and Food Sciences

Debrecen, 2023

1. BACKGROUND AND OBJECTIVES OF THE DOCTORAL DISSERTATION

The predicted increase in food demand from 59% to 98% by 2050, when there will be 9 billion people on the planet (DURO et al., 2020). The issue of food security for the planet's rapidly increasing population is humanity's largest global challenge. The United Nations defines food security as "when all people at all times have physical, social, and economic access to sufficient, safe, and nutritious food that meets their food preferences and dietary needs to maintain an active and healthy life" (WORLD FOOD SUMMIT, 1996). This challenge is compounded primarily by global climate change, limited water resources, and the need for safer and better quality commodities using fewer chemicals and environmentally friendly practices. The development of irrigation technology, as well as monitoring and sensing technologies related to it, through the development of precision agriculture technology, is a critical element for climate adaptation (TAMÁS, 2001). Non-destructive measurements can be carried out using a variety of remote sensing methods without the actual use of active ingredients and without the need to physically modify the materials. The collection of spectral data enables the rapid development of information about the study region and provides the basis for reliable monitoring. Thus, crop yield estimation is important for agricultural planning and ensuring the nation's food production security in crop monitoring systems by providing decision-makers early indication of agricultural production (FRITZ et al., 2019). The intensity of extended droughts in Hungary has increased recently and varies from region to region. Improving water management as efficiently as possible is essential when agricultural production in our nation is to develop at the correct rate. The control of Variable Rate Irrigation (VRI) has emerged as an important and relevant problem from across the world as a consequence of irrigation development developments. VRI can improve quality and production while decreasing water, fertilizer, agrochemical, and energy use (LI et al., 2021).

The primary objective of my research is to evaluate and develop the water flow parameters of precision irrigation technology within the framework of the water scarcity-food security-watershed level linkages and climate adaptation linkages. Through modeling based on validated spectral data series and non-invasive measurement methods, I designed to evaluate the plant-soil-water relations, hydrological processes, and water-household relations of the crop production space at the regional and farm level in the Tisza catchment, both in the field and horticultural production.

Water flow problems can be first and foremost observed in the reduction of biomass and crop quantity and quality, therefore crop monitoring allows the quantification of stress effects on

arable crops. In our country, besides maize, I aimed to develop monitoring of yield loss of wheat, our most important arable crop. I applied and developed a methodological basis for stress monitoring systems for field crops caused by water scarcity and drought, using different satellite time series data and calculated vegetation indices under both regional and field conditions.

Several agrotechnical tools can be used to combat the stress effects of drought and water scarcity in both field and horticultural conditions. One of the most effective agrotechnical tools against drought is irrigation. Domestic irrigation systems are outdated in most places and are not capable of VRI, therefore, in my thesis, I evaluated the technical parameters of a linear irrigation system equipped with a first overflow VRI in our country.

The use of micro-irrigation systems in intensive horticultural production is a well-established and indispensable practice. However, apple production, which is the dominant one in domestic fruit production, is complemented by the use of hail net agrotechnical protection, the impact of which on the microclimate and the water flow of the plant is not sufficiently explored. Therefore, I aim to conduct a complex assessment of the effects of hail netting on apple orchard water turnover and to develop a rapid spectral assessment methodology for water stress effects. Water turnover is also influenced by soil factors, the possibility of rapid monitoring of which is essential from a crop management point of view. Among several soil parameters, I aimed to develop a rapid, non-invasive methodology for measuring organic matter content, which has a significant impact on water and nutrient cycling.

I have developed the following research objective based on what is generally accepted:

1. Develop an agricultural drought monitoring and yield estimation system in the Tisza watershed area
 - Development of a yield monitoring system based on MODIS NDVI data calibrated with crop yield data at the regional level,
 - Development of a yield monitoring system at the farm level based on Landsat 8 satellite data calibrated with crop yield data.
2. Evaluation of the water depth of a linear irrigation system controlled by VRI technology, one of the first in Hungary, based on dispersion uniformity and accuracy
 - Testing irrigation homogeneity: assessing the degree of under- and over-irrigation
 - Evaluation of longitudinal water allocation between zones,
 - Evaluation of cross-water allocation between zones.

3. Evaluation of the impact of hail net use on apple orchard water balance
 - Quantifying the differences in microclimate,
 - Canopy thermography, pigment content, canopy water potential, stress, and dry matter content,
 - Evaluation of effects on physical parameters of the crop.
4. Development of a methodology for non-invasive assessment of abiotic stress effects in apple orchards and its adaptation to Early Gold and Golden Reinders based on spectral characteristics of chlorophyll content in the orchard in the 400-1000 nm wavelength range.
5. Development and domestic adaptation of a rapid non-invasive soil organic matter estimation methodology based on plain soil samples in the VIS-NIR (400-2500 nm) wavelength range.

2. MATERIAL AND METHODS

2.1. Description of the research areas

Tisza watershed area

In my research, the samples needed to develop regional and farm-level crop estimation systems and soil organic matter content estimation models are located in the Tisza watershed. The study area is the plain part of an international watershed, the Tisza watershed, which is the most important wheat and maize growing region in the Carpathian Basin. Temperature, solar radiation, and soil moisture are three climatic factors that influence vegetation development. In addition to meteorological data, the soil heterogeneity of the plain areas influences crop production. This makes it important to estimate yields in the area, intervene over time, and test the soil quality appropriately.

Irrigated arable land

A real-time eco potential measurement methodology for a water-saving precision irrigation system for an 85-ha arable field of Bátortrade KFT was developed during the research. The first VRI-equipped linear irrigation system in the country was installed in 2020, with the test period starting in 2020 and 2021. Analyzing the geometry and geography of the area, in general, there are only a few meters of elevation difference across the whole area, mostly with a northeast slope, and the slope is less than 5% in 96.93% of the area. The physical characteristics of the soil are sand, which is less sensitive to irrigation intensity.

Apple orchard cultivation area

The evaluation of the impact of the use of hail nets on the water flow in apple orchards was carried out at the Pallag Horticultural Experimental Station of the Agricultural Research Institutes and Agricultural Extension of the University of Debrecen. The experiments were carried out in an intensively cultivated Early Gold and Golden Reinders apple orchard protected by micro-irrigation and hail net. There are 100 individuals in each row of the apple orchard, the first 50 of which are protected by hail net. The orchard is located on sandy soils with extreme water balance, which makes the stress of water shortage and heat a particularly high risk (NAGY, 2015).

2.2. Development of a crop estimation system based on satellite imagery

2.2.1. Development of a crop estimation system based on MODIS satellite images

I downloaded MOD13Q1V6 pictures for the seven counties in the Tisza watershed area from <https://earthexplorer.usgs.gov> to process the MODIS satellite images. I utilized TerrSet and ArcGIS geospatial software based on TAMÁS et al., (2015) and NAGY et al., (2018) to process the downloaded satellite images. The calibration was performed by setting up linear regression with the average wheat yield (t/ha) values available from the Central Statistical Office for the years 2000-2016, and the results were validated with data for the years 2017-2018. I used a remotely sensed time series of at least 6 years to maximize accuracy based on literature data for yield analysis (DEMPEWOLF et al., 2014; NAGY et al, 2018).

2.2.2. Development of a crop estimation system based on Landsat 8 satellite images

Landsat 8 satellite photos for the growing season 2013–2019 were downloaded for this study from <https://earthexplorer.usgs.gov/>. The data of wheat yield averages (t/ha) from 26 field plots of the Landsat 8 satellite images were provided during the 2013-2019 period by the Research Institute of Agricultural Research and Farming Karcag (from 2021 MATE Karcag Research Institute) of the University of Debrecen. Data collection, processing, calibration, and validation are still only some of the steps required for data processing and yield estimation. In my research, I set up yield estimation models using NDVI and SAVI.

2.3. Pivoting linear irrigation system

A unique pivoting lateral moving sprinkler irrigation machine was installed in the field. The total structural length of the irrigation machine is 209.09 m including the end console. The maximum water demand of the system was 180 m³/h and the minimum water demand was depending on the aim of the VRI. Out of the 118 nozzles, 62 nozzles operated only in lateral movement mode, 48 nozzles operated only in pivot mode, and 8 nozzles in the center of the irrigator operated in both linear and pivot modes. The nozzle type selected for the experiment was the standard low-pressure Nelson O3030 Orbitor black nozzle.

2.3.1. Measurement of irrigation water depth

The VRI performance of the irrigation system was measured in grids, along the irrigation system progress directions, and along the lateral pipeline to evaluate the water distribution of the linear irrigation system. The measurements in the grids were made to model a management zone with a constant irrigation rate. The catch cans were placed at a height of 50 cm in a 6*4

grid with a distance of 5 m. The irrigation test was carried out in the direction of the irrigation machine's development to verify the longitudinal transition of water discharge between two irrigation zones and to establish the absolute minimum length of the treatment zone. The zones planned water depths were 5 and 10 mm. The 20th catch cans were used to calculate the design line between zones. Four zones were set transversely along the pipeline with pulse timing, cycle times of 25, 50, 75, and 100%, and a maximum planned water depth of 10 mm to analyze the accuracy of irrigation in the various treatment zones. I placed 40 catch cans in a straight line every meter for the cross and longitudinal zone transition measurements.

2.3.2. Method for measuring irrigation uniformity

In this study, the coefficient of Christiansen-uniformity (CUc%) (CHRISTIANSEN, 1941; TAKÁCS et al., 2018), the low quarter distribution uniformity (DU%), and the coefficient (CV) of variation were used. In addition to calculating the uniformity coefficients, I also examined the distribution of irrigation water applied to the irrigated area by calculating the percentage of under and over-irrigated areas based on the placement of the grid nets. The distribution of applied irrigation water was plotted and calculated in Surfer 15 (Golden Software, Inc, Golden, Colorado).

2.4. The effects of hail net as an agrotechnological factor

Field surveys were carried out in 2016, 2019 and 2020. Field surveys were carried out weekly between 9-10 am, and in 2020, bi-weekly surveys were carried out between 9-2 pm with hourly surveys. During each field survey, I measured the temperature and relative humidity with a Testo 175 H1 instrument to investigate the positive effects of the hail net on the microclimate. During the canopy temperature measurements, 14 thermographic surveys were carried out with the HEXIUM PYROLATER-12 Thermo camera in 2016. 15-15 hail net protected and non-protected individuals were surveyed for each of the two apple cultivars studied. The thermographic images of the canopy were taken at a height of 1-2 m from the shaded west side to reduce the adverse effect of direct sunlight. Based on preliminary research in orchards by NAGY, (2015), the period between 9-11 h is recommended for thermographic surveys. The thermal image was preprocessed to extract only the canopy values of the apple trees to remove background soil and air pixels, after which the average canopy temperature could be determined. In addition to evaluating the thermographic data, I also monitored canopy water balance using a Scholander Pressure Chamber Leaf Water Potential Meter (Pump-Up Chamber, PMS Instrument Company). I selected 20 individuals per species, 10 from areas protected by

hail nets and 10 from areas not protected by hail nets. Measurements were carried out six times in July and August 2019 between 9 and 10 am, and in 2020 from 07.21.07 to 14.00 every two weeks with 3 to 3 samples. The measurement methodology was based on FULTON et al. (2014).

To ensure homogeneity of sampling, leaf samples were taken from 1.2 m height from the middle part of a branch to determine the pigment content of the selected trees, following NEMESKÉRI et al. (2009). Sampling was carried out between 9 and 10 h, for which 15-15 apple trees were selected from hail net protected and non hail net protected areas for both species. Leaf samples were stored and transported refrigerated at 4 °C and measured in the laboratory within 6 h. Samples were destained with 80 % acetone and 1 g quartz powder for homogeneity. After extraction, the suspensions were centrifuged at 3000 rpm for 3 min in a Hettich ROTOFIX 32A and the clear solution was transferred to a 2.5 ml quartz vial. The absorbance of the solution was measured with a SECOMAN Anthelie Light II at 470, 644, and 663 nm. The chlorophyll content of the samples was determined according to the equation published by DROPPA et al. (2003). Carotenoid values were determined according to the equation of LICHTENTHALER and WELLBUM (1983). The dry matter content was determined in parallel with the laboratory determination of the pigment content using conventional gravimetric methods. Soil moisture content was monitored during each field survey in parallel with the sampling. Samples were taken from a depth of 30 cm and the moisture content was measured by a gravimetric method similar to the leaf dry matter content and expressed as a percentage by weight.

To measure plant stress, I used a chlorophyll fluorimeter of the OS30p+ (Opti-Sciences) type. The OS30p+ was developed to measure chlorophyll fluorescence using the Fv/Fv, Fv/Fo dark adaptation protocols, and the Fv/x test. Healthy plants have an Fv/Fm of 0.79-0.84 (MAXWELL and JOHNSON, 2000). Lower values indicate plant stress. For the tests, I selected 10 to 10 trees from hail net protected and non-protected areas for each of the two cultivars tested. Stress measurements of the apple cultivars were carried out biweekly from 07.21.2020 between 9-14 h with hourly surveys from the shaded side of the selected individuals.

Physical parameters of apple yield were determined on 8 August 2022 from selected hail net protected and unprotected Early Gold and Golden Reinders apple trees. From each selected tree, 20 fruit were randomly picked and transported to the DE MÉK Water and Environmental Management Institute laboratory, where fruit width and height were measured with a caliper, and fruit weights were determined on an analytical balance.

2.5. Methodology for spectral assessment of abiotic stress on the apple orchard

Sampling was carried out twice a week between 9 and 10 am from 7 July 2019 to 29 August 2019. During each measurement period, 30 samples were collected from each of the two apple varieties tested. For the spectral data collection of leaf samples, I used an AvaSpec 2048 spectrometer with a wavelength range of 400-1000 nm and an accuracy of 0.6 nm. Statistical analysis of the results was performed using SPSS software. To identify the wavelength with the highest factor weight, I used PCA with varimax rotation to identify the chlorophyll-sensitive wavelength.

2.6. Spectral estimation methodology for soil organic matter content

2.6.1 Soil sampling and development of spectral-based models for estimating soil organic matter content

To develop a spectral estimation methodology for soil organic matter content, I collected a total of 90 soil samples in 2020 from 0-20 cm depth, of which 60 soil samples were used to calibrate the developed models and 30 samples to validate the models. Sampling locations were randomly determined in the Tisza catchment. Soil organic carbon analysis was performed at the Agricultural Centre of DE MÉK using the Walkley-Black method. Spectral profiles were measured with two separate laboratory spectrometers between 400 and 2500. Statistical analysis of the results was performed using SPSS software. To identify the wavelength with the largest factor weight, I used PCA with varimax rotation to identify the SOC-sensitive wavelength (ALLEN, 2017). In addition to PCA, I also examined the standard deviations (SD) of the spectral features to select the wavelengths where the deviations were the largest, indicating the potential variability of the SOC.

3. RESULTS

3.1. Crop yield estimation based on MODIS NDVI time series data

Wheat yield estimation was done by regression of harvested yields and time series derived from MODIS NDVI data. Linear regression values were calculated using NDVI and KSH yields obtained for 10 and 26 June based on the preliminary studies and methodology of NAGY et al. (2018), which yielded $R^2=0.458$ for 10 June and $R^2=0.567$ for 26 June (Figure 1). The coefficient of determination values are moderately strong for further evaluation.

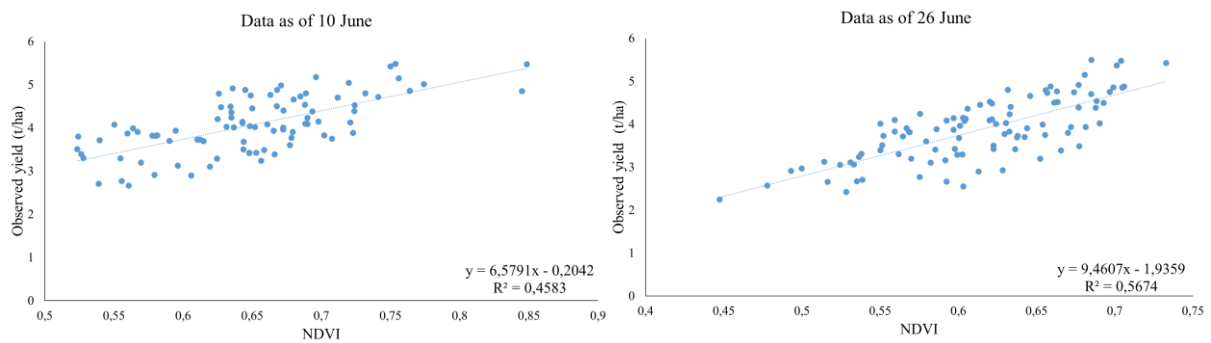


Figure 1. Yield prediction models

Using the mean relative and absolute deviations of the estimated value from the true value, I examined the relationships between estimated yield and harvested yield values at 1, 3, and 6-year intervals for all years and counties studied. The relative 1-year average deviation of the estimated value from the true value on 10 June was 1.951%, with an absolute deviation of 10.58%. The relative 3-year average deviation of the estimated value from the true value was 2.455%, with an absolute deviation of 10.85%. The average relative deviation of the 6-year estimated value from the fair value was 2.478% and the absolute deviation was 10.46%. As of 26 June, the relative average deviation of the 1-year estimated value from fair value was -0.722%, with an absolute deviation of 11.79%, the relative average deviation of the 3-year estimated value from fair value was -0.476%, with an absolute deviation of 11.73%. The relative average deviation of the 6-year estimated value from the true value was -0.471%, while the absolute deviation was 11.58%. The negative values obtained indicate that the models tend to underestimate the values. The relative deviation values were lower than the accepted threshold of 5% in the literature (FERENCZ et al., 2004). From 2000 to 2018, the RMSE error of the reliability of the estimation models for the 7 counties studied averaged 0.491 t/ha (NRMSE=12.19%) for June 10 and 0.545 t/ha (NRMSE=13.33%) for June 26. NSE was used

as a global measure of model performance, which gave an estimate of $NSE = 0.799$ using the NDVI values for the models.

3.2. Crop yield estimation based on LANDSAT 8 NDVI and SAVI time series data

Wheat yield estimation was done by regressing harvested yield values and NDVI and SAVI time series of 6 different peak periods derived from Landsat 8. Vegetation indices derived from Landsat 8 data were applied and tested to produce wheat yield estimates and forecasts. The peak wheat season is observed in May and early June, followed by the ripening period and then the harvest period in early July. Therefore, to estimate the wheat yield, I collected NDVI and SAVI data from day 120 to day 190 (30 April to 9 July). The NDVI and SAVI indices showed the highest peak values between days 138 and 150 (18 May to 30 May) (NDVI: 0.461 ± 0.077 ; SAVI: 0.837 ± 0.338). The significance and strength of the correlations between the IPs and wheat yield varied with the variation in NDVI and SAVI values. The coefficients of determination for both VIs were highest ($R^2 > 0.6$) between days 138 and 167 (18 May and 16 June). This interval corresponded to the period from BBCH 41 to 71. The relationship between wheat yield and SAVI values was stronger than for NDVI, suggesting that SAVI is a better predictor of wheat yield. To better understand the yield estimation algorithms defined, I chose the results of regression analysis to interpret the characteristics of NDVI and SAVI-based models in sections BBCH 41, BBCH 59, and BBCH 71. To further validate the estimation models and calculate their accuracy, I used the average wheat yields harvested in the study area between 2018 and 2019. I used NSE as a global measure of model performance, which gave a strong estimation value of $NSE = 0.722$ based on NDVI values and $NSE = 0.915$ based on SAVI values using the models. The coefficients of determination for wheat showed values of more than 60% for NDVI and 70% for SAVI during the peak phenological period. Although, the accuracy of the estimates for NDVI varied from 0.255-0.452 t/ha (5.139%-9.301%) based on the RMSE and NRMSE values of the estimator models. The best estimation accuracy was obtained with models derived from the early ripening periods. For SAVI, the accuracy of the estimated values varied from 0.177-0.239 t/ha (3.347-4.646%), indicating a better performance of the estimator models. To evaluate the overall accuracy of the VI-based estimator models, the estimated yield values for the entire most sensitive periods were averaged and compared with the harvested yield values. The RMSE of the NDVI-based estimator model was 0.357 t/ha (NRMSE: 7.336%) and the RMSE of the SAVI-based estimator model was 0.191 t/ha (NRMSE 3.867%). The average relative deviation (-1.072%) showed that NDVI underestimated the harvested yield values. The SAVI-based estimates showed a smaller but positive deviation

(0.466%) from the harvested values. The average absolute deviation between estimated and harvested yield data was also larger for the NDVI-based forecast (about 8.515%) compared to an absolute deviation of 4.132% for the SAVI-based forecast. Based on the results obtained, only the accuracy of the NDVI-based estimates exceeded the 5% threshold, which is generally accepted as good (FERENCZ et al., 2004).

3.3. Testing irrigation water application with a new linear irrigation system

3.3.1 Evaluation of water application in a management zone with a constant irrigation rate

Tables 1 and 2 summarize the combined results of the irrigation tests for the irrigation volume CV, CUc, and DU, and the over- and under-irrigation characteristics in a model farming zone at a constant irrigation rate.

Table 1. Irrigation uniformity results of grid experiment

	water depth (mm)	CUc%	DU%	CV%	Under irrigated area (m ²)	Under irrigation %	Overirrigated area (m ²)	Overirrigation %
First measurement	10,03 ± 0,641	95,25	90,97	6,435	8,555	3,810	0,007	0,030
Second measurement	9,692 ± 1,065	92,10	87,74	10,96	0,485	0,131	2,244	0,601
Third measurement	9,757 ± 0,945	92,31	87,18	9,681	0,795	0,211	0,211	0,414

Table 2. Irrigation accuracy results of grid experiment

	MAE (mm)	MBE (mm)	NRMSE%
First measurement	0,475	-0,031	6,235
Second measurement	0,691	0,310	11,32
Third measurement	0,679	0,255	8,112

To summarize the results, all tests proved that constant rate irrigation was uniform and homogeneous in the modeled management zone, although the second two measurements gave slightly lower CUc%, DU%, and thus higher CV% values compared to the first measurement. This is probably due to the weather conditions. While the weather during the first measurement was completely calm at the site, wind gusts of 10-13 km/h from the northeast were observed

during the second and third measurements, which may explain the lower values of CUC% and DU%.

3.3.2. Evaluation of longitudinal transition of water application between zones

Border water allocation is likely to be affected by the different planned irrigation levels in the farming zones. However, it is important to know the width of the boundaries between zones in the direction of the irrigator's travel, as this will determine the minimum adjustable length of the management zone for the VRI. The longitudinal transition between zones was continuous and homogeneous between rainfall gauging pans 14 and 26, which is a 12 m wide boundary between management zones in the direction of irrigator travel. This is probably due to the application radius of the irrigators (Figure 2).

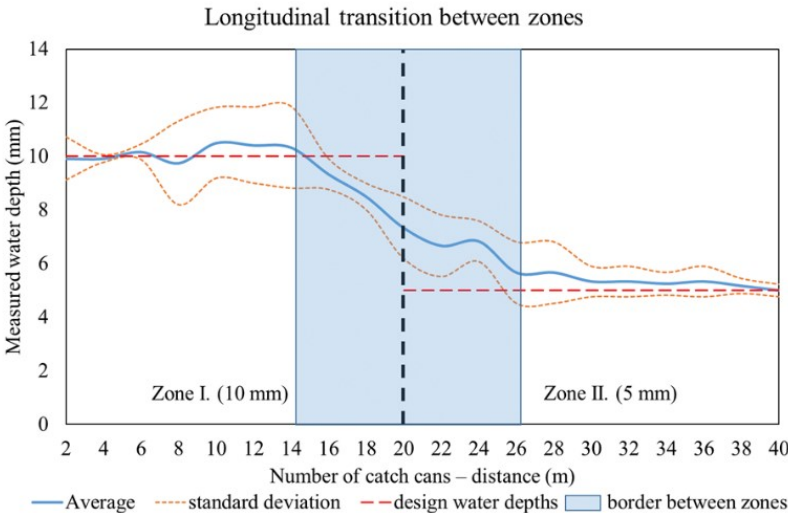


Figure 2. Evaluation of the transition between irrigation zones

3.3.3. Evaluation of the uniformity of irrigation in different management zones along the pipeline

The water distribution characteristics of VRI systems are a key indicator for assessing irrigation uniformity in different management zones (Table 3).

Table 3. Results of the accuracy of irrigation in different management zones along the pipeline

No. of the zone	design water depths (mm)	CUC%	DU%	CV%
1	2,5	81,36	81,36	20,26
2	5	85,94	78,28	17,31
3	7,5	92,81	88,42	9,355
4	10	92,98	90,75	8,439

The combined results of the average of the measured water depths, NRMSE, MAE, and MBE for the water discharge of the four VRI zones along the pipeline at different planned water discharges are plotted in Table 4. Significant differences in water depths were found between the treatment zones, indicating that the VRI system performed well and that the planned irrigation levels of the treatment zones were different in all cases. The deviation from the target level was analyzed to assess the accuracy of irrigation in each treatment zone. For all treatment zones, the measured water depth in the catchment basins was slightly less than the designed irrigation water depth.

Table 4. Results of the accuracy of irrigation in different management zones along the pipeline

No. of the zone	design water depths (mm)	N	average measured water depths (mm)	MAE (mm)	MBE (mm)	NRMSE%
1	2,5	20	2,417 ^a	0,458	0,042	21,97
2	5	20	4,934 ^b	0,645	0,146	11,52
3	7,5	20	7,050 ^c	0,625	0,313	7,021
4	10	20	9,200 ^d	0,767	0,633	5,519

There is no statistical difference between populations marked with the same letter ($p > 0.05$).

3.4. Influence of hail net as an agrotechnical tool on the apple orchard

3.4.1. Effect of hail net on microclimate

I first analyzed the micro climatological effects of the hail net on changes in air temperature ($^{\circ}\text{C}$) and relative humidity (%). In 2019, I measured 26.58 ± 2.192 $^{\circ}\text{C}$ in the hail net protected individuals, 2.911 % lower than the 27.37 ± 2.201 $^{\circ}\text{C}$ measured in the non hail net protected orchard. The difference was not significant ($p = 0.150$). There was a significant difference between the relative humidity of 71.52 ± 15.43 % in the orchard protected by hail nets and 69.33 ± 16.50 % in the orchard not protected by hail nets ($p = 0.0001$). On average, hail nets increased the relative humidity in the apple orchard by 3.16 %. Following this trend, the temperature in 2020 was 26.21 ± 1.712 $^{\circ}\text{C}$ for the plants protected by hail nets, whereas 27 ± 1.625 $^{\circ}\text{C}$ was observed for plants not protected by hail nets. There was a difference of 3.055% between the results, with no significant difference between them ($p=0.058$). Relative humidity values were $58.50 \pm 4.767\%$ in the hail net protected area and $56.30 \pm 4.329\%$ in the non hail net protected area, with no significant difference between them ($p=0.167$). The hail net increased the relative humidity by an average of 3.804 %. In 2019, thanks to micro-irrigation, the difference between the average soil moisture values was negligible (0.484%, $p = 0.776$)

(11.07 ± 2.181 m/m% for those protected by hail nets and 11.06 ± 2.367 m/m% for those not protected by hail nets), resulting in a homogeneous water supply for the entire orchard. The more rainy weather in 2020 was also observed in soil moisture values, with higher soil moisture results at all measurement dates compared to 2019. The minimum soil moisture value was 6% and the maximum soil moisture value reached 20% in the area protected by the hail net. The effect of the hail net was more dominantly observed for hourly variations, with soil moisture content values up to 4-5% higher in the hail net protected area.

3.4.2. Evaluation of the effect of hail net on water supply based on thermographic data

The thermographic data showed that the average canopy temperature of apple orchards protected by hail nets was lower in most cases. Overall, the canopy temperature of the protected apple trees (25.69 ± 2.022 °C) was significantly ($p = 0.006$) 7.283 % lower than the mean canopy temperature of the unprotected individuals (27.71 ± 2.328 °C). My results indicate that the use of hail nets has different effects on the two apple species. For Early Gold, the average leaf temperature of the protected stands was 26.80 ± 2.444 °C, 2.825 % lower than the average leaf temperature of the non-protected stands (27.58 ± 2.465 °C), with no significant difference between the results ($p = 0.326$). For Golden Reinders, there was a significant difference between leaf temperatures ($p = 0.017$). The mean leaf temperature of the hail net protected individuals (24.59 ± 2.491 °C) was 11.66 % lower than the 27.84 ± 3.381 °C of the non hail net protected apple trees. In a comparison of Golden Reinders, canopy temperatures showed a difference of 8.919% greater for the canopy protected by hail netting than Early Gold. This suggests that the use of hail netting has a more beneficial effect on the canopy temperature of Golden Reinders. To analyze the effect of hail netting in more detail, I evaluated the differences in canopy temperature at each measurement time. Even though Early Gold is located in a more inland part of the orchard (row 3) than Golden Reinders (row 2), the average canopy temperature of Early Gold trees was similar or lower, 1.335°C higher than Golden Reinders trees. This is probably due to the more thermally sensitive characteristics of the Early Gold variety.

3.4.3. Effects of hail net on foliage water potential

The water content of plants causes tension or negative pressure in the plants, resulting in negative values of plant water potential (FULTON et al., 2014). The average water potential of orchards protected by hail nets (-8.5 ± 1.846 bar) is 20.80% higher than the average water potential of orchards not protected: -10.8 ± 2.769 bar. However, there was no significant difference ($p = 0.399$) due to the large variation in water potential values. Similar results were

obtained when evaluating the varieties separately. In 2019, the water potential values of Early Gold trees protected by hail nets were 18.67% higher, indicating a better water supply to the trees. The difference was not significant ($p = 0.837$): the water potential was -8.5 ± 2.502 bar in the hail net protected orchards and -10.4 ± 2.983 bar in the non hail net protected orchards. In 2020, during the Early Gold measured between 9 and 10 h, hail net protected orchards had an average water potential value of -6.8 ± 1.955 bar, while non hail net protected orchards had a higher water potential value of -7.5 ± 2.422 bar, with no significant correlation observed ($p=0.095$). However, in 2019, for Golden Reindeer, there was a significant difference between the water potential values of the protected and non-protected orchards ($p = 0.030$). The difference was 22.78 %: higher water potential values (-8.7 ± 1.307 bar) were measured in the hail net protected orchard, while in the non hail net protected orchard, the water potential was -11.2 ± 2.633 bar. In 2020, a positive effect of hail netting was observed in Golden Reinders measured between 9-10 h, similar to Early Gold, where protected individuals gave water potential values of -6.2 ± 1.475 bar and non-protected individuals gave -7.9 ± 2.324 bar, with no significant correlation observed ($p=0.385$). In 2020, the hourly water potential of the varieties was examined, and for both Early Gold and Golden Reinders, a steady decrease in water potential was observed over time. The effect of the hail net is best illustrated by the results from 17.08.2020 for both of the 2 varieties studied. In the case of Early Gold, it was observed that the water potential value decreased from -4.7 ± 0.291 bar in the morning to -9.3 ± 0.587 bar at 14 h. In the area not protected by hail nets, it was observed that a higher water potential value of -5.2 ± 0.299 bar was obtained at 9 h, which decreased to -10.70 ± 1 bar at 14 h. A similar trend was observed in the Golden Reindeer, where the water potential value for the individuals protected by the hail net at 9 h was -4.7 ± 0.588 bar, almost doubling to -10.70 ± 1.533 bar at 14 h. The positive effect of the use of hail nets was observed at all measurement times over time, with the water potential value in the unprotected area at 9 h being -5.3 ± 1 bar, which decreased to -14.20 ± 4.544 bar at 14 h.

3.4.4. Effects of hail net on the dry matter content

In some plant physiology literature, the water status of the plant is expressed as the water potential of the leaf, whereas in my research I observed the possible effect of the hail net on the absolute dry matter content. A lower dry matter content value may reflect a more favorable water supply. The results showed that the dry matter content of the leaves of the orchard protected by hail nets (34.11 ± 3.238 m/m %) was 4.761 % lower than that of the orchard without hail nets (35.81 ± 4.458 m/m %), but the difference was not significant ($p = 0.119$).

When evaluating the varieties separately, a significantly lower dry matter content of 7.635% ($p = 0.033$) was found for Golden Reinders (36.17 ± 4.458 m/m% for the non hail net protected and 33.41 ± 3.755 m/m% for the hail net protected). However, a smaller (1.830%) and non-significant ($p = 0.406$) difference in dry matter content of the orchards were found for Early Gold (34.80 ± 3.442 m/m% and 35.45 ± 5.104 m/m%, respectively).

3.4.5. Effects of hail net on the pigment content

The chlorophyll content (2874 ± 283.6 $\mu\text{g/g}$) of the orchard protected by hail nets was 10.24 % higher than that of the orchard without hail nets (2607 ± 412.8 $\mu\text{g/g}$). However, the difference between the results was not significant ($p=0.066$). Early Gold had a canopy chlorophyll content of 3070 ± 400.2 $\mu\text{g/g}$ in the hail net protected area, which was 11% higher than in the non hail net protected orchard (2766 ± 449.1 $\mu\text{g/g}$). However, no significant difference was observed ($p=0.071$). Similar results were also observed for Golden Reiders apple trees, with the average chlorophyll content of apple trees protected by hail nets (2725 ± 316.1 $\mu\text{g/g}$) 11% higher than in the non hail net protected orchard (2455 ± 445.6 $\mu\text{g/g}$). The difference between the results obtained was not significant ($p=0.236$). Comparing the cultivars, Golden Reinders showed the same difference in chlorophyll content with hail netting as Early Gold. This suggests that the application of hail nets does not cause a difference in chlorophyll content between the varieties. Another photosynthetically active pigment is the carotenoid. The use of hail netting resulted in a significant ($p = 0.004$) increase (16.41 %) in the carotenoid content of the apple canopy (562.6 ± 47.56 $\mu\text{g/g}$ when using hail netting, 483.3 ± 62.70 $\mu\text{g/g}$ in the area not protected by hail netting). The difference was 18 % and also significant ($p = 0.026$) for Early Gold (595.3 ± 70.28 $\mu\text{g/g}$ in the area protected by hail nets and 505.7 ± 73.72 $\mu\text{g/g}$ in the area not protected by hail nets). The carotenoid content of the canopy of Golden Reinders protected by hail netting was 533.1 ± 49.21 $\mu\text{g/g}$, which was significantly ($p = 0.009$) 16.24 % higher than the carotenoid content of 458.6 ± 65.01 $\mu\text{g/g}$ of apple trees not protected by hail netting. Comparing cultivars, Golden Reinders showed a 2.15% greater difference in leaf carotenoid content in the presence of ice netting than Early Gold. This suggests that the use of hail netting has a slightly more beneficial effect on the carotenoid content of Golden Reinders.

3.4.6. The effect of hail net on foliage stress values

The fluorometer's status indicator is the Fv/Fm ratio, which is a parameter characterizing the status of photosynthetic electron transport. In parallel with the stress measurement, I measured the stand climate, where I observed that the Fv/Fm values decreased with time, and thus with

the continuous increase of temperature the stress effects were more and more pronounced in the apple trees under study. During the study period, the highest temperature (27.90 °C for the hail net protected and 28.95 °C for the non hail net protected) and the lowest humidity (47.75 % for the hail net protected and 45.50 % for the non hail net protected) were observed on 04.08.2020 between 13-14 h in both the hail net protected and non hail net protected areas. A negative correlation was observed for temperature and humidity (-0.79 in the hail net protected area and -0.85 in the non hail net protected area). Based on MAXWELL and JOHNSON (2000), Fv/Fm values between 0.79 and 0.84 indicate healthy, stress-free vegetation, with lower values indicating plant stress. The Fv/Fm value of the orchard protected by hail nets was 0.73 ± 0.033 , which is 4.107% higher than the Fv/Fm value of 0.70 ± 0.031 for orchards not protected by hail nets. There was a significant difference between the results ($p=0.004$). Observing the varieties separately, Early Gold individuals protected by hail nets were less exposed to stress than those not protected by hail nets. The highest Fv/Fm value was observed on 21.07.2020. The highest stress values were observed between 9 and 11 h in hail net protected individuals (Fv/Fm = 0.76 ± 0.022), no significant difference was observed between the observed values ($p=0.199$). However, the positive effect of hail netting was observed, with Fv/Fm values 3% higher for Early Gold protected by hail netting (hail netting: 0.71 ± 0.701 , non hail netting: 0.65 ± 0.098), with a significant difference between the results ($p=0.001$). For Golden Reindeer, a 9% higher Fv/Fm was observed in the hail net protected individuals (hail net protected: 0.71 ± 0.701 , hail net not protected: 0.65 ± 0.098), with no significant difference between the results ($p=0.151$). The highest Fv/Fm result was obtained between 9-10 h on 21/07/2020 with a result of 0.77 ± 0.022 , which also gave the highest Fv/Fm value in the period studied. A significant difference was observed between the data ($p=0.004$). Based on the values obtained, it can be concluded that the increase in temperature influences the stress values of the vegetation, which can be detected by a rapid, non-invasive field method. Moreover, the obtained values support the positive effect of using hail nets against heat stress.

3.4.7. Impact of hail net on apple yields

When examining the fruits, I observed that the width of the fruits of trees protected by hail nets was 3% higher than the width of the fruits of trees not protected by hail nets (protected by hail nets: 6.433 ± 0.667 cm, not protected by hail nets: 6.255 ± 0.501 cm). A significant difference was observed between the results ($p=0.035$). The height of the fruit of trees protected by hail nets (6.381 ± 0.790 cm) was 2% greater than the height of the fruit of trees not protected by hail nets (6.261 ± 0.711 cm), a significant difference was observed between them ($p=0.0007$). When

fruit weight was examined, 168.1 ± 52.22 g of the fruit of the trees protected by hail nets was 15% higher than 143.7 ± 27.61 g of the unprotected trees. A significant difference was observed between the results ($p=0.031$). The dry matter content of the fruits was 4% higher in the hail net protected individuals than in the non hail net protected individuals (hail net protected: 26.90 ± 5.931 g, non hail net protected: 25.81 ± 7.688 g), with no significant difference between the observed values ($p=0.201$). When the fruit values of the varieties were examined separately, a similar trend was observed, which is presented in Table 5.

Table 5. Physical parameters of the fruits of apple varieties

		Width (cm)	Height (cm)	Weight (g)	Dry matter content (g)
Early Gold	Protected with hail net	$6,422 \pm 0,817$ b	$6,405 \pm 0,766$ a	$176,6 \pm 64,66$ a	$29,10 \pm 5,934$ a
	Non-protected with hail net	$6,278 \pm 0,415$ a	$6,115 \pm 0,490$ a	$147,2 \pm 25,45$ a	$25,86 \pm 9,680$ a
Golden Reinders	Protected with hail net	$6,440 \pm 0,496$ b	$6,655 \pm 0,969$ b	$159,5 \pm 35,53$ b	$27,78 \pm 7,099$ a
	Non-protected with hail net	$6,237 \pm 0,591$ a	$6,134 \pm 0,657$ a	$140,1 \pm 29,85$ a	$23,08 \pm 5,391$ a

There is no statistical difference between populations marked with the same letter ($p > 0.05$).

3.4.8. Relationships between water balance parameters

In addition to the analysis of the effect of the hail net on water balance and pigment variables, correlation analyses were also performed between those values of variables, which showed significant differences at specific measurement times. As evidence, in the case of chlorophyll and carotenoids a significant positive correlation can be detected ($r = 0.943$, $p = 0.004$). The canopy temperatures and chlorophyll content were inversely proportional to each other ($r = -0.491$, $p = 0.033$). Inverse proportionality was also observed in the correlation between carotenoid and canopy temperature values due to the reduced heat stress, however, the correlation was not significant ($r = -0.328$, $p = 0.383$). There was a significant inverse relationship between dry matter content and canopy temperature ($r = -0.718$, $p = 0.007$). The above can be explained by the fact that the increased canopy temperature due to the warmer and drier microclimate of the orchards without hail net decreased the photosynthetic activity, as well as, the moisture content of the foliage. Hail net reduces heat stress by bringing canopy temperature closer to the temperature optimum for its photosynthesis (RAVEH et al., 2003). The positive effect of the hail net on water balance is also supported by the fact that the higher water potential values are associated with higher chlorophyll and carotenoid content. This is

supported by a significant positive correlation between chlorophyll and water potential values ($r = 0.644$, $p = 0.015$) and a significantly moderately strong correlation between carotenoid and water potential values ($r = 0.660$, $p = 0.017$). There is a significant but weak correlation between dry matter and water potential values as well ($r = 0.289$, $p = 0.006$).

3.5. Spectral assessment of abiotic stress and development of chlorophyll prediction models

The lowest chlorophyll content was 1828 $\mu\text{g/g}$ and the highest was 4576 $\mu\text{g/g}$. In my results, it was observed that leaves with high chlorophyll content showed a reflectance value between 8-10%, which shows an increasing reflectance with decreasing chlorophyll values. At low chlorophyll values of 1800-2700 $\mu\text{g/g}$, a reflectance value of 11-12% was observed. The maximum reflectance of carotenoids was measured in the 520-580 nm wavelength range, which gave a low reflectance value of around 12% at high chlorophyll content. It is observed that the reflectance value increases proportionally with decreasing chlorophyll content for carotenoid content. The carotenoid at low chlorophyll content interval values gave a reflectance value of 17-18%. Thus, plant stress can be detected in the wavelength range of 500-700 nm with high reflectance values. To further investigate the spectral characteristics of the leaf samples, the relative standard deviation values of the reflectance (%) data were divided into several groups based on chlorophyll content (1800-2700 $\mu\text{g/g}$, 1800-3100 $\mu\text{g/g}$, 1800-4000 $\mu\text{g/g}$, 1800-4600 $\mu\text{g/g}$). Low standard deviation (up to 520 nm \pm 30 nm) was observed in the low chlorophyll content groups. The standard deviation of reflectance increased in parallel with chlorophyll content. Therefore, this range may be suitable for plant maturity studies. The peak of the standard deviation is prominent at 670 nm due to the absorption characteristics of chlorophyll measured in this wavelength range, sensitive at high chlorophyll content. It is observed that the standard deviation of reflectance values calculated in the wavelength ranges 550 nm, 670 nm, and 700 nm is pigment sensitive. This sensitivity decreases due to an increase in absorbance with increasing carotenoid content. Thus, this spectral characteristic disappears with increasing carotenoid content. PCA resulted in five principal components. Based on the factor weights of the first component, the two largest variations in reflectance are observed in the 556 and 710 nm wavelength range. Two minima in the factor weight were observed, of which the 800 nm range was used together with the 556 and 710 nm ranges to construct the chlorophyll estimation indices. I created three indices in my research: $\text{Index}_1 = (\lambda_{800} - \lambda_{710}) / (\lambda_{800} + \lambda_{710})$ which was based on a linear regression with a strong regression value $R^2 = 0.561$ ($p = 0.000$). The $\text{Index}_2 = (\lambda_{800} - \lambda_{710}) / \lambda_{556}$ model showed a strong correlation with $R^2 = 0.506$ ($p = 0.000$). The $\text{Index}_3 = (\lambda_{800} -$

$\lambda_{556}/\lambda_{710}$ model also showed a strong regression with $R^2=0.560$ ($p=0.000$). The Chlorophyll_{model1} operating in the 400-1000 nm wavelength range had NSE=0.601 MBE=84.59 $\mu\text{g/g}$ and MAE=243.4. The Chlorophyll_{model2} had NSE=0.595, MBE=62.59 $\mu\text{g/g}$, and MAE=246.9 $\mu\text{g/g}$. Using the Chlorophyll_{model3} was NSE=0.601, MBE=91.48 $\mu\text{g/g}$, and MAE=244.6 (Figure 3).

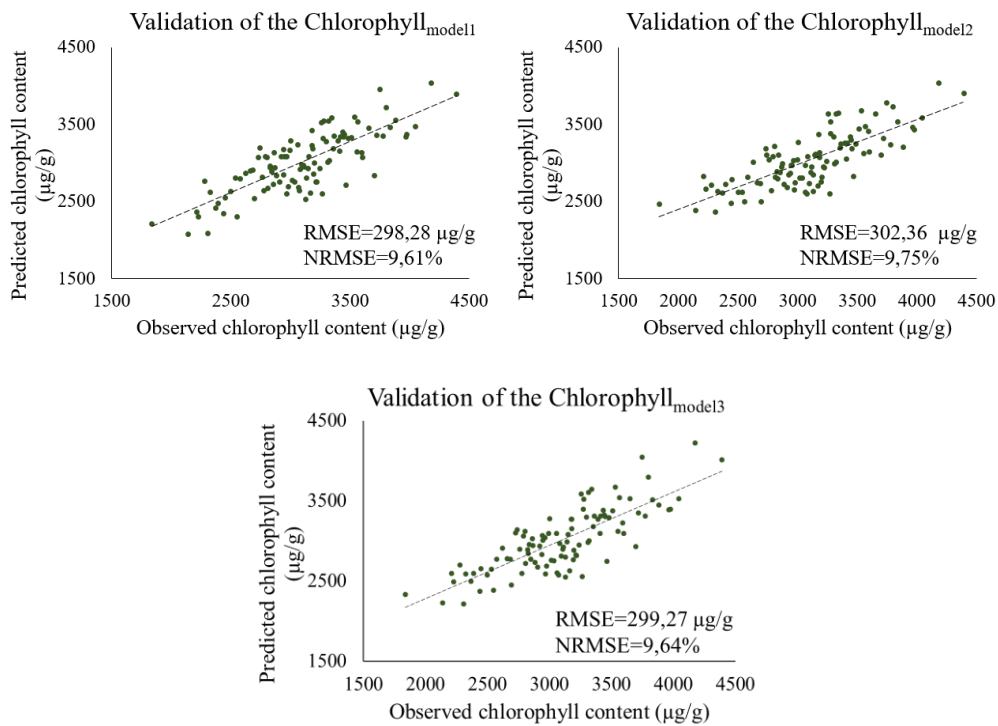


Figure 3. Accuracy of predicted models based on validation of chlorophyll models

3.6. Development of soil organic content estimation indices based on spectral analyses

The reflectance profiles of the dry soil samples were evaluated in the 400-2500 nm range. On average, the reflectance increases linearly with longer wavelength. The reflectance of the soil samples varied from 9-14% at shorter wavelengths, reaching 34-39.5% at 1000 nm. The standard deviation curve of the reflectance profile took a parabolic shape. The minimum reflectance value was observed at short wavelengths (400-430 nm) due to the high absorption of the soil. It then reaches a maximum in a relatively broadband in the wavelength range 600-800 nm and then decreases again up to 1000 nm. Based on the SD, the largest variation in reflectance was in the 650-750 nm range. In the 1000-2500 nm range, on average, an increase in the reflectance is observed with longer wavelengths, reaching a partial peak between 2150-2300 nm, followed by a slight decrease. Three decreases were observed at 1420 nm, 1930 nm,

and 2210 nm, resulting in valleys in the reflectance curves. The first two dips are characteristic of the water absorption bands of the soil spectrum. The PCA resulted in five main components. Based on the factor weights of the first component, the largest variance in reflectance was in the 580-600 nm range, so I used the average of the reflectance factors at these wavelengths as the numerator of the first spectral index, but because of the differences and discrepancies identified earlier, I considered the 960-970 nm range to be less sensitive to SOC, and therefore calculated $\text{Index}_1 = \lambda_{580-600} / \lambda_{960-970}$. The first SOC model ($\text{SOC}_{\text{model1}}$) was based on linear regression with a moderately strong regression value $R^2=0.475$ ($p=0.000$). The first prominence of the PCA curves in the NIR range was observed at 1020-1040 nm, which I combined with the second wavelength difference at 1900-2100 nm. From the two observed differences I formed the $\text{Index}_2 = \lambda_{1020-1040} / \lambda_{1900-2100}$ model. The $\text{SOC}_{\text{model2}}$ showed a strong correlation ($R^2=0.611$, $p=0.000$). The $\text{SOC}_{\text{model3}}$ was determined from the factor weights of the starting and ending wavelength ranges in the NIR. Based on this, a difference was observed in the 1000-1010 nm range, and a minimum of the factor weights was observed in the 2420-2500 nm wavelength range, which is less sensitive to SOC. Based on the results obtained, the generated $\text{Index}_3 = \lambda_{1000-1010} / \lambda_{2420-2500}$ showed a strong regression value, $R^2=0.562$ ($p=0.000$). Based on the results of the PCA curve, I created the $\text{SOC}_{\text{model4}}$ from the increasing factor weight data of the first VIS range and the increasing factor weight data of the third NIR range $\text{Index}_4 = \lambda_{640-660} / \lambda_{2200-2300}$. The $\text{SOC}_{\text{model4}}$ was based on linear regression with a moderately strong regression value $R^2=0.493$ ($p=0.000$). The $\text{SOC}_{\text{model1}}$, which also operated in the 400-1000 nm wavelength range, had $\text{NSE}=0.561$. Two models were developed to estimate SOC in the NIR wavelength range. The $\text{SOC}_{\text{model2}}$ with the strongest regression coefficient resulted in an $\text{NSE}=0.855$, which confirms the best reliability of the model estimation. The $\text{SOC}_{\text{model3}}$ used had an $\text{NSE}=0.725$. The $\text{SOC}_{\text{model4}}$ had an estimation accuracy of $\text{NSE}=0.727$ (Figure 4).

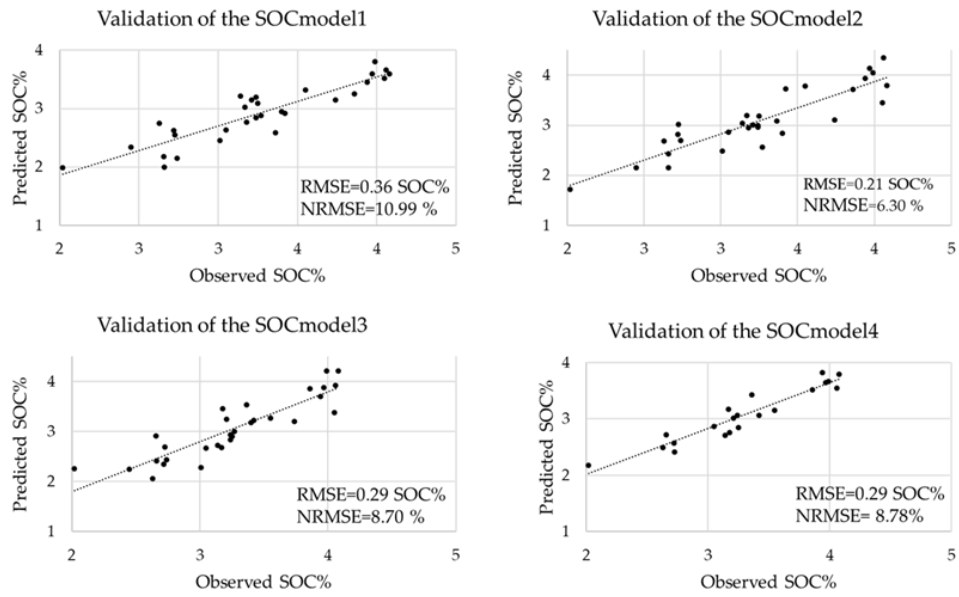


Figure 4. The accuracy of prediction models based on the validation of SOC models

4. NEW SCIENTIFIC RESULTS OF THE THESIS

1. Based on satellite time series data, I developed regional and farm-level wheat yield estimation models in the Tisza watershed. Based on MODIS NDVI time series data, I found that the estimator models at the regional level are the most accurate based on six years of data (MPE = -0.471-2.478 %, MAPE= 10.46-11.58 %, NRMSE= 12.19-13.33 t/ha, NSE=0.799). Based on Landsat 8 NDVI and SAVI time series data, I found that at the farm level, the error of NDVI-based estimator models is below 10% (MPE= -1.072%, MAPE= 8.515%, NRMSE= 5.139-9.301 %, NSE=0.722), while the error of SAVI based estimator models is below 5% (MPE= 0.466%, MAPE= 4.132%, NRMSE= 3.347-4.646 %, NSE=0.915).
2. I found that controlled water delivery using site-specific irrigation technology mounted on a reversible linear irrigation system can be achieved homogeneously (CUC=93.22%, DU=88.63%) and with accurate rates (MAE= 0.615 mm, MBE= 0.185 mm, NRMSE= 8.555 %).
3. I found that, in sandy soils and under lowland climatic conditions, the hail net protected cover has a positive effect on the water balance of Early Gold and Golden Reinders apple orchards. As a result of lower temperature (-2.980%) and higher humidity (3.488%), the canopy temperature of apple trees protected by hail net was 7.283% lower, and leaf dry matter content was 4.761% lower than that of unprotected apple trees. The average water potential of the hail net orchards was 20.80%, chlorophyll 10.24%, carotenoid 16.41%, Fv/Fm 4.107%, fruit width 3%, height 2%, weight 15%, and dry matter 4% higher than the unprotected fruit trees.
4. Three chlorophyll content estimation models were developed for Early Gold and Golden Reinders apple cultivars using a non-invasive measurement methodology in the wavelength range 400-1000 nm. Among the models, the model based on $Index_1 = (\lambda_{800} - \lambda_{710}) / (\lambda_{800} + \lambda_{710})$ ($R^2=0.561$, RMSE=298.3 $\mu\text{g/g}$, NRMSE=9.616%, NSE=0.601, MBE=84.59 $\mu\text{g/g}$ és MAE=243.4 $\mu\text{g/g}$) is the most accurate for the rapid, non-destructive analysis and estimation of chlorophyll content of Early Gold and Golden Reinders apple cultivars.
5. I developed four soil organic matter content estimation models based on a non-invasive measurement methodology in the wavelength range of 400-2500 nm. Among the developed estimator models, $Index_2 = \lambda_{1020-1040} / \lambda_{1900-2100}$ (RMSE=0.219 SOC%, NRMSE=6.301%, NSE=0.855) is the most accurate for rapid non-invasive assessment of soil organic matter content.

5. THE PRACTICAL USE OF THE RESULTS

1. MODIS NDVI time series data images with the monitoring system developed, approximate results can be obtained up to 4 weeks before wheat harvest.
2. Landsat 8 NDVI and SAVI time series data images with the monitoring system developed, approximate results can be obtained up to 6 weeks before wheat harvest. In the case of SAVI, the accuracy of the estimated values shows a better performance of the prediction models.
3. The application of the developed non-invasive soil organic matter prediction models allows for obtaining fast and detailed information on soil organic matter content from a large number of samples. Based on spatial data, even the number of samples required for accredited measurements can be optimized, thus reducing sampling and analysis costs.
4. Black hail net in apple orchards has a positive effect on the water balance of heat and drought-sensitive apple varieties, especially Golden Reinders. Their adaptation to heat and water stress is also reflected in the physical parameters of the yield. Overall, the use of a hail net is not only effective against ice damage but also attenuates abiotic stress effects on apple fruit. Further studies on the quality of the fruit are recommended.
5. The use of non-invasive chlorophyll content prediction models adapted to apple cultivars allows us to obtain fast and detailed information on the chlorophyll content of individuals in an orchard based on a large number of samples, which can also be a better stress indicator compared to existing vegetation indices.
6. The spray uniformity of a linear irrigation system with variable rate irrigation technology is homogeneous with minimal under- and over-irrigation. In addition, taking into account the transient effect of the boundaries between zones, a treatment zone shall be greater than 12 m longitudinally.

6. REFERENCES

1. Allen, M.: 2017. The sage encyclopedia of communication research methods. Thousand Oaks, CA: SAGE Publications, 1438-1440.
2. Christiansen E. J.: 1941. The uniformity of application of water by sprinkler systems. *Agricultural Engineering*. 22(3): 89–92
3. Dempewolf, J.- Adusei, B.- Becker-Rehef, I.- Hansen, M.- Potapov, P.- Khan, A.- Barker, B.: 2014. Wheat Yield Forecasting for Punjab Province from Vegetation Index Time Series and Historic Crop Statistics. *Remote Sens.*, 6, 9653–9675.
4. Droppa, M.- Erdei, S.- Horváth, G.- Kissimom, J.- Mészáros, A.- Szalai, J.- Kosáry, J.: 2003. Plantbiochemistry and plantphysiology in practice (In Hungarian: Növénybiokémiai és növényélettani gyakorlatok) Budapest, 88.
5. Duro, J.-Lauk, C.- Kastner, T.- Erb, K. H.- Haberl, H.: 2020. Global inequalities in food consumption, cropland demand, and land-use efficiency: A decomposition analysis. *Global Environmental Change*. 64. 102124.
6. Ferencz, C.- Bognár, P.- Lichtenberge, J.-Hamar, D.- Tarcsai, G.- Timár, G.- Molnár, G.- Pásztor, S.- Steinbach, P.- Székely, B. (2004) Crop yield estimation by satellite remote sensing. *Int. J. Remote Sens.*, 25, 4113–4149.
7. Fritz, S. - See, L.- Bayas, J.C.L.- Waldner, F.- Jacques, D.- Becker-Reshef, I.- Whitcraft, A. - Baruth, B.- Bonifacio, R.- Crutchfield, J.: 2019. A comparison of global agricultural monitoring systems and current gaps. *Agric. Syst.*, 168, 258-272
8. Fulton, A.- Grant, J.- Buchner, R.- Conell, J. (2014): Using the Pressure Chamber for Irrigation Management in Walnut, Almond and Prune (ANR Publication 8503 University of California), pp. 1–27.
9. Li, X.- Zhao, W.- Li, J.- Li, Y.: 2021. Effects of irrigation strategies and soil properties on the characteristics of deep percolation and crop water requirements for a variable rate irrigation system. *Agricultural Water Management*, 257, 107143.
10. Lichtenthaler, H.K.- Wellbum, A.R.: 1983. Determinations of total carotenoids and chlorophylls a and b of leaf extracts in different solvents. *Biochem. Soc. Trans.* 603, 591–592.
11. Maxwell, K.- Johnson, G.: 2000. Chlorophyll fluorescence - a practical guide. *J Exp Bot* 51: 659-668. *Journal of experimental botany*. 51.
12. Nagy, A.- Fehér, J.- Tamás, J.: 2018. Wheat and maize yield forecasting for the Tisza river catchment using MODIS NDVI time series and reported crop statistics. *Comput. Electron. Agric.*, 151, 41–49.
13. Nagy, A.: 2015. Thermographic Evaluation Of Water Stress In An Apple Orchard. *Journal of multidisciplinary engineering science and technology* 2: 8 pp. 2210–2215.
14. Nemeskéri, E.- Sárdi, É.- Kovács-Nagy, E.- Stefanovits Bányai, É.- Nyéki, J.- Szabó, T.: 2009. Studies on the drought responses of apple trees (*Malus domestica* Borkh.) grafted on different rootstocks. *Int. J. Hortic. Sci.* 15 (1-2), 29–36.
15. Raveh, E.- Cohen, S.- Raz, T.- Yakir, D.- Grava, A.- Goldschmidt, E.E.. 2003. Increased growth of young citrus trees under reduced radiation load in a semi-arid climate. *J. Exp. Bot.* 54 (381), 365–373.
16. Takács S.- Helyes L.- Bíró T.- Pék Z.: 2018. Variable Rate Precision Irrigation Technology for Deficit Irrigation of Processing Tomato. *Irrigation and Drainage*. 68, 234-244.
17. Tamás, J.: 2001. Precíziós mezőgazdaság. Szaktudás Kiadó Ház ZRT.
18. Tamás, J.-Nagy, A.- Fehér, J.: 2015. Agricultural biomass monitoring on watersheds based on remote sensed data. *Water Sci. Technol.*, 72, 2212–2220.
19. *World Food Summit: 1996, Rome Declaration on World Food Security*



Registry number: DEENK/367/2023.PL
Subject: PhD Publication List

Candidate: Andrea Szabó
Doctoral School: Doctoral School of Nutrition and Food Sciences
MTMT ID: 10068754

List of publications related to the dissertation

Foreign language Hungarian books (1)

1. Nagy, A., Bódi, E., **Szabó, A.**, Tamás, J.: Advanced technologies of precision irrigation. Debreceni Egyetem Mezőgazdaság-, Élelmiszertudományi és Környezetgazdálkodási Kar, Debrecen, 106 p., 2021. ISBN: 9789634903277

Hungarian book chapters (2)

2. **Szabó, A.**, Adeniyi, O. D., Tamás, J., Nagy, A.: Búzatermés előrejelzés lehetőségének értékelése Landsat 8 idősoros adatok alapján.
In: Az elmélet és a gyakorlat találkozása a térinformatikában XI. : Theory meets practice in gis. Szerk.: Molnár Vanda Éva, Debreceni Egyetemi Kiadó, Debrecen, 249-256, 2020. ISBN: 9789633188866
3. **Szabó, A.**, Adeniyi, O. D., Tamás, J., Nagy, A.: Wheat yield prediction based on MODIS NDVI time series data in the wider region of a cereal processing plant.
In: Innovációs kihívások a XXI. században : LXI. Georgikon Napok konferenciakötete. Szerk.: Pintér Gábor, Csányi Szilvia, Zsiborács Henrik, Pannon Egyetem Georgikon Kar, Keszthely, 407-415, 2019. ISBN: 9789633961308

Hungarian scientific articles in Hungarian journals (4)

4. **Szabó, A.**, Tamás, J., Nagy, A.: Precíziós öntözőberendezés szóráségyenletességének értékelése.
Hidrol. Közlöny. 101 (1), 74-79, 2021. ISSN: 0018-1323.
5. **Szabó, A.**, Tamás, J., Nagy, A.: A jégvédő háló használatának hatásai az alma gyümölcsös vízháztartására és lombozatának pigment tartalmára.
Kertgazdaság. 52 (3), 3-16, 2020. ISSN: 1419-2713.
6. Nagy, A., Tamás, J., **Szabó, A.**, Gálya, B., Fehér, J.: Mezőgazdasági aszály monitoring és aszály előrejelzés távérzékelés adatok alapján a Tisza vízgyűjtőn.
Hidrol. Közlöny. 99 (4), 60-68, 2019. ISSN: 0018-1323.





7. Szabó, A., Tömöri, F., Vad, A., Tamás, J., Nagy, A.: Precíziós öntözéstechnológia alkalmazásának és kialakításának vizsgálata.
Int. J. Eng. Manag. Sci. 4 (4), 239-248, 2019. EISSN: 2498-700X.
DOI: <http://dx.doi.org/10.21791/IJEMS.2019.4.27>.

Foreign language scientific articles in Hungarian journals (2)

8. Szabó, A., Tamás, J., Nagy, A.: Preliminary studies to evaluate the use of spectral data in monitoring of apple orchard parameters.
Acta Agrar. Debr. 2, 37-41, 2022. ISSN: 1587-1282.
DOI: <http://dx.doi.org/10.34101/actaagrar/2/8454>
9. Szabó, A., Kubicza, K., Tamás, J., Nagy, A.: Effect of hail net on the water potential of an apple orchard.
Acta Agrar. Debr. 2, 109-113, 2020. ISSN: 1587-1282.
DOI: <http://dx.doi.org/10.34101/ACTAAGRAR/2/3728>

Foreign language scientific articles in international journals (6)

10. Szabó, A., Tamás, J., Kövesdi, Á., Nagy, A.: Evaluation of new pivoting linear-move precision irrigation machine = Evaluation d'une nouvelle machine d'irrigation de precision a mouvement lineaire pivotant.
Irrig. Drain. [Epub ahead of print], 1-12, 2023. ISSN: 1531-0353.
DOI: <http://dx.doi.org/10.1002/ird.2850>
IF: 1.9 (2022)
11. Szabó, A., Tamás, J., Nagy, A.: An Irrigation Homogeneity Assessment of a Variable Rate Sprinkler Irrigation.
Acta Horticulturae et Regiotecturae. 24 (1), 8-11, 2021. ISSN: 1335-2563.
DOI: <http://dx.doi.org/10.2478/ahr-2021-0002>
12. Szabó, A., Adeniyi, O. D., Tamás, J., Nagy, A.: Assessment of a Yield Prediction Method Based on Time Series Landsat 8 Data.
Acta Horticulturae et Regiotecturae. 24 (1), 12-15, 2021. ISSN: 1335-2563.
DOI: <http://dx.doi.org/10.2478/ahr-2021-0003>
13. Szabó, A., Tamás, J., Nagy, A.: The influence of hail net on the water balance and leaf pigment content of apple orchards.
Sci. Hortic. 283, 1-8, 2021. ISSN: 0304-4238.
DOI: <http://dx.doi.org/10.1016/j.scienta.2021.110112>
IF: 4.342
14. Nagy, A., Szabó, A., Adeniyi, O. D., Tamás, J.: Wheat Yield Forecasting for the Tisza River Catchment Using Landsat 8 NDVI and SAVI Time Series and Reported Crop Statistics.
Agronomy-Basel. 11 (4), 1-13, 2021. EISSN: 2073-4395.
DOI: <http://dx.doi.org/10.3390/agronomy11040652>
IF: 3.949





15. **Szabó, A.**, Tamás, J., Adeniyi, O. D., Nagy, A.: Wheat yield prediction based on MODIS NDVI time series data in the wider region of a cereal processing plant.
Nat. Res. Sustain. Develop. 9 (2), 193-202, 2019. ISSN: 2066-6276.
DOI: <http://dx.doi.org/10.31924/nrsd.v9i2.036>

List of other publications

Foreign language international book chapters (1)

16. Nagy, A., **Szabó, A.**, Gálya, B., Tamás, J.: Real-time spectral information to measure crop water stress for variable rate irrigation scheduling.
In: Precision agriculture '21. Ed.: John V. Stafford, Wageningen Academic Publishers, Wageningen, 427-433, 2021. ISBN: 9789086863631

Hungarian scientific articles in Hungarian journals (1)

17. Tamás, J., Bódi, E., Gálya, B., **Szabó, A.**, Fehér, J., Nagy, A.: Integrált városi hidrológiai modell módszertani alapjai vízgyűjtő-gazdálkodási tervezés támogatásához.
Hidrol. Közöny. 100 (3), 56-63, 2020. ISSN: 0018-1323.

Foreign language scientific articles in Hungarian journals (1)

18. **Szabó, A.**, Juhász, C., Gálya, B., Kövesdi, Á., Tamás, J., Nagy, A.: Combined traffic control of irrigation on heterogeneous field.
Acta Agrar. Debr. 1, 187-190, 2022. ISSN: 1587-1282.
DOI: <http://dx.doi.org/10.34101/actaagrar/1/10369>

Foreign language scientific articles in international journals (2)

19. Gálya, B., Nagy, A., Juhász, C., Riczu, P., **Szabó, A.**, Blaskó, L., Tamás, J.: Identification of inland-excess water patches based on LIDAR and Sentinel 1 data.
Nat. Res. Sustain. Develop. 10 (2), 188-199, 2020. ISSN: 2066-6276.
DOI: <http://dx.doi.org/10.31924/nrsd.v10i2.054>
20. **Szabó, A.**, Tamás, J., Nagy, A.: Spectral evaluation of the effect of poultry manure pellets on pigment content of maize (*Zea mays* L.) and wheat (*Triticum aestivum* L.) seedlings.
Nat. Res. Sustain. Develop. 9 (1), 70-79, 2019. ISSN: 2066-6276.
DOI: <http://dx.doi.org/10.31924/nrsd.v9i1.025>

Foreign language abstracts (3)

21. Nagy, A., Bódi, E., **Szabó, A.**, Fehér, Z. Z., Tamás, J.: Assessment of UAV-based LiDAR and photogrammetry data in crop morphology monitoring for advanced irrigation.
In: EGU Gallileo Conferences : A European vision for hydrological observations and experimentation, European Geosciences Union, Munchen, GC8-Hydro-103, 2023.





22. Nagy, A., Fehér, Z. Z., **Szabó, A.**, Bódi, E., Magyar, T., Tamás, J.: Management of alternative water resources for variable rate irrigation - a Hungarian case study.
In: EGU General Assembly 2023 : HS5.3 : Strategies for allocations of scarce water resources and technologies for improving water productivity in agriculture : Posters on site, European Geosciences Union, Munchen, EGU23-5592, 2023.
23. Nagy, A., **Szabó, A.**, Juhász, C., Gálya, B., Kövesdi, Á., Tamás, J.: Combined traffic control of irrigation on heterogeneous field.
In: Poster Proceedings of the 13th European Conference on Precision Agriculture. Eds.: J. V. Stafford, G. Milics, Magyarországi Precíziós Gazdálkodási Egyesület, Budapest, 31-32, 2021. ISBN: 9786150120171

Total IF of journals (all publications): 10,191

Total IF of journals (publications related to the dissertation): 10,191

The Candidate's publication data submitted to the iDEa Tudóstér have been validated by DEENK on the basis of the Journal Citation Report (Impact Factor) database.

11 August, 2023

